


RESEARCH ARTICLE



N-Acetylcysteine relieving hydrogen peroxide-induced damage in granulosa cells of sheep

Hao Chen ^{*}, Jine Wang^{*}, Bingzhu Zhao, Yahua Yang, Chongfa Yang, Zhijie Zhao, Xiaona Ding, Yang Li, Taojie Zhang, Zhaxi Yingpai, and Shengdong Huo

College of Life Science and Engineering, Northwest Minzu University, Lanzhou, Gansu, China

ABSTRACT

Sheep ovarian granulosa cells (GCs) play a unique role in the ovary. Damage to GCs can affect the normal development of oocytes. The oxidative stress model was constructed by H_2O_2 to study the biological changes. Specifically, pathological characteristic was assessed by immunohistochemistry (IHC), while signaling pathway was studied using western blot, quantitative RT-PCR, and immunofluorescence. The results showed that the oxidative damage model was successfully constructed by $200 \mu\text{mol/LH}_2\text{O}_2$ for 12 h. NAC can protect the proliferation of GCs under H_2O_2 -induced oxidative stress and reduce apoptosis. It can also promote the secretion of E_2 and P_4 by GCs and reduce the inflammatory response of GCs. NAC can enhance the expression of NRF2, PI3K and Akt. These findings suggest that NAC alleviates H_2O_2 -induced oxidative stress injury through NRF2/PI3K/AKT signaling pathways. Provide ideas for studying the poor quality of mammalian oocytes.

Highlights

- The molecular mechanism of NAC anti-oxidation through NRF2/HO-1.
- The molecular mechanism of NAC anti-oxidation through PI3K/AKT.
- NAC has antioxidant capacity on granulosa cells.

ARTICLE HISTORY

Received 30 August 2024
Revised 13 March 2025
Accepted 20 March 2025

KEYWORDS



Granulosa cells;
N – acetylcysteine; oxidative
stress; sheep

Introduction


The ovary of mammals is the most dynamic organ in adult females, which is closely related to the reproductive performance of animals. Follicle is the most basic structural and functional unit of mammalian ovary [1]. The mature follicles are composed of oocytes, cumulus cells, ovarian GCs, TCs and follicular fluid. Follicular maturation and ovulation are intricate physiological processes [2]. During these processes, a rapid increase in metabolites can decrease the activity of antioxidant enzymes, leading to elevated levels of reactive oxygen species (ROS) [3]. Under normal conditions, The production and digestion of ROS are transformed into a dynamic equilibrium state, with an appropriate ROS concentration supporting ovarian development and ovulation [4]. However, excessive ROS [5] levels can trigger oxidative stress, promote cell damage, activate apoptosis pathways, and contribute to abnormal follicular atresia, affecting oocyte quality and reproductive outcomes [6].

In mammalian ovaries, GCs proliferate first, and when the number of proliferation reaches a certain

level, oocytes begin to develop [7]. In the process of follicular growth and development, there are many regulatory networks between GCs and follicles [8,9]. The proliferation of GCs involves the whole process of follicular growth and development. GCs regulate follicular development by secreting steroid hormones, cytokines, growth factors, etc., providing a good growth environment for follicular development. There is a gap link between GCs and oocytes [7,10]. Through cell gap junctions, oocytes secrete factors such as BMP15 and GDF9 to regulate the proliferation and differentiation of GCs. Through gap junctions, oocytes can also excrete metabolic waste generated inside. GCs can provide and transmit small molecules of nutrients, vitamins, calcium ions, metabolic precursors and signal transduction molecules required for oocytes through gap links. The FSH receptor on the surface of the GCs membrane can bind to FSH, activate the cAMP pathway, promote the expression of aromatase genes, make estrogen synthesized in large quantities, and further promote follicular growth. With the continuous

CONTACT Shengdong Huo  huoshd@xbmu.edu.cn  College of Life Science and Engineering, Northwest Minzu University, Lanzhou, Gansu 730030, China

^{*}These authors contributed equally to this work and should be considered as co-first authors.

 Supplemental data for this article can be accessed online at <https://doi.org/10.1080/19336918.2025.2484182>

© 2025 The Author(s). Published by Informa UK Limited, trading as Taylor & Francis Group.

This is an Open Access article distributed under the terms of the Creative Commons Attribution License (<http://creativecommons.org/licenses/by/4.0/>), which permits unrestricted use, distribution, and reproduction in any medium, provided the original work is properly cited. The terms on which this article has been published allow the posting of the Accepted Manuscript in a repository by the author(s) or with their consent.

development of follicles, the volume and number of GCs increase. Under the action of LH, GCs undergo luteinization, maintain the secretion of progesterone by luteal cells, and further regulate oocyte maturation and ovulation [11].

When animal cells are cultured in vitro, the appropriate concentration of NAC solution is added to the culture medium, which can increase the proliferation activity of germ cells and inhibit their apoptosis, thus delaying the aging of animals and increasing their life span. That is because N-acetylcysteine (NAC), as an effective antioxidant, can scavenge free radicals in cells and indirectly synthesize reduced glutathione (GSH) [12], thereby mitigating oxidative stress injuries in animals. Studies have demonstrated that NAC can inhibit oxidative stress in various cell cultures and animal models [13].

Therefore, this study aims to investigate the effects of varying concentrations of NAC on GCs proliferation [14], apoptosis, ROS levels, hormone secretion, and related gene and protein expression [15]. By employing the PI3K/AKT inhibitor LY294002 [16], the molecular mechanisms will be explored. Additionally, the relationship between cellular antioxidant capacity and NRF2/PI3K/AKT signaling pathways will be investigated to determine whether NAC alleviates H₂O₂-induced oxidative stress damage through these pathways [17].

Materials and methods

Cell processing and identification

In this study, the ovaries of healthy ewes aged about 2 years old were isolated and cultured from the slaughterhouse in Wushengyi Town, Gansu Province. Extract follicular fluid from ovarian follicles with a diameter of approximately 3–8 mm into a tube. Filter the follicular fluid through a 100 nm filter, then centrifuge at 1500 r/min to collect the precipitate. The cells were resuspended in DMEM containing 10% fetal bovine serum. Observe cell morphology and culture at 37°C, 5% CO₂. FSHR immunofluorescence staining was performed when the cell adhesion reached 70%–80%. The cells were fixed in 4% paraformaldehyde at room temperature for 30 min, the immunofluorescence permeabilization solution was used to penetrate the membrane at room temperature for 30 min, and the immunostaining blocking solution was blocked at room temperature for 1 h. Cells were incubated with 1:200 concentration of FSHR at 4°C overnight. The cells were incubated with 1:1000 anti-rabbit secondary antibody at room temperature in the dark for 1 h. Blank control was

only incubated with secondary antibody. DAPI staining was performed in dark for 5 min.

Construction and treatment of GCs oxidative damage model

The primary GCs were inoculated into 96-well plates (density of 1×10^4 cells/well), and the blank group was set up: only 100 µL medium was added; control group: 90 µL cell suspension and 10 µL culture medium were added; experimental group: 90 µL cell suspension was added. The cells were pre-cultured in 5% CO₂ incubator at 37°C for 12 h, and 10 µL of H₂O₂ with final concentrations of 100, 150, 200 and 250 µmol/L was added to the experimental groups, respectively. Then the cells were cultured in 5% CO₂ incubator at 37°C for 6, 12, 24 and 36 h, respectively. After that, 10 µL of cck-8 solution was added to each well and incubated for 2 h. The absorbance at 450 nm was measured by microplate reader. When the cell survival rate was as low as about 50%, the determined H₂O₂ concentration and induction time were the optimal damage concentration and time for the construction of GCs oxidative damage model. Cells were observed under the microscope to determine the cell status. When the cell confluence reached 80% or more, the cells were digested with 0.25% trypsin and cultured in a 1:2 ratio for passage. The cells were treated with control group, NAC group (100 µmol/L), H₂O₂ group (200 µmol/L), and NAC (100 µmol/L) + H₂O₂ (200 µmol/L) group. Each group had three biological replicates.

CCK-8 assay

The cells were seeded in 96-well plates, 1×10^4 cells per well, and the culture medium was discarded after 6 h of culture. The control hole, test hole and blank hole were set up, and NAC solution holes with concentrations of 0, 50, 100, 500 and 1000 µmol/L were added respectively, and only culture medium holes were added, with 3 replicates in each group. Cells in each group were cultured for 24, 48 and 72 h, and 10 µL CCK-8 solution was added to each well. After incubation at 37°C for 2 h, the absorbance at 450 nm was measured by microplate reader. Cell proliferation activity was calculated according to the formula. Cell viability (%) = $[(A(\text{plus}) - A(\text{empty})) / (A(0\text{plus}) - A(\text{empty}))] \times 100$. A(plus): with cells, CCK-8 solution, affecting drugs; a(empty): with medium, CCK-8 solution, no cells; a(0plus): with cells, CCK-8 solution, no effect on the drug.

Flow cytometry

Add 90 μ L cell suspension to 96-well plates. After pre-incubation in a 5% CO₂ incubator at 37°C for 12 h, 10 μ L of H₂O₂ with final concentrations of 100, 150, 200 and 250 μ mol/L was added to the experimental groups, respectively. The cell culture supernatant was collected to centrifuge tubes, and the cells were washed twice with PBS. The stained cell suspension was transferred to a flow tube, and the data were detected and analyzed by flow cytometry.

ROS determination

The DCHFDA stock solution was diluted with serum-free medium to a final concentration of 10 μ M. The cells were slowly washed with PBS for 3 times, then the diluted dye was added. The images were taken under a fluorescence microscope.

Oxidative stress indicators determination

The levels of glutathione (GSH) and malondialdehyde (MDA), as well as the activity of superoxide dismutase (SOD), were determined using commercial kits. Following treatment, the GCs were collected and washed three times with ice-cold PBS. The resulting pellet was then homogenized with pre-cooled PBS at 4°C or in an ice bath. Subsequently, the homogenate was centrifuged at 10,000 rpm at 4°C for 10 minutes, and the supernatant was collected as the sample for testing. The assays were conducted according to the instructions provided with the GSH, SOD, and MDA detection kits (Biyuntian, Shanghai, China).

ELISA assay

The culture medium was collected in 1.5 mL centrifuge tubes. The supernatant was obtained after centrifugation at 2500 rpm for 20 minutes. The concentrations were measured by the kits (Shanghai, Mlbio, China). Each group consisted of three biological replicates.

Immunofluorescence staining

The isolated cells were inoculated into 24-well plates, and the cells adhered to 80%. The cell culture medium was discarded and washed with PBS buffer for 3 times, 2 min each time. Add 250 μ L paraformaldehyde to fix for 30 min, discard the fixative, and wash with PBS buffer for 3 times, 2 min each time. Add 250 μ L 0.2% Triton X-100, incubate at room temperature for 15 min, discard the liquid and wash with PBS buffer 3

times, 2 min each time. The diluted primary antibody was added to each well, and the same amount of PBS buffer was added to the negative control well. The cells were incubated at 4°C for 12 h, and washed with PBS buffer for 3 times, 5 min each time. Each well was added with 500 μ L of diluted secondary antibody and placed in a dark room. After incubation at room temperature for 3 h, it was washed with PBS buffer for 3 times, 5 min each time. In the dark room, 200 μ L DAPI staining solution was added to each well, incubated at room temperature for 1 min, and washed with PBS buffer for 3 times, 5 min each time. Observed and photographed by a fluorescence microscope in a dark room.

RNA isolation, reverse transcription, and quantitative RT-PCR

Total RNA was extracted using the Trizol method (SOLEIBO, Beijing, China), and the concentration and purity of the RNA samples were assessed using a NanoDrop One/OneC spectrophotometer. RNA samples with D260/D280 values between 1.8 and 2.0 were chosen for cDNA synthesis, which was performed using the Prime SCRIPT TMRT kit (Takara, Beijing, China) with 1 μ g of high-purity RNA. qRT-PCR was conducted using SYBR PreMix Ex Taq TM II (Takara, Beijing, China) and a real-time PCR system (Bio-Rad, Hercules, CA, USA). The reaction conditions were as follows: pre-denaturation at 95°C for 3 minutes, followed by denaturation at 95°C for 10 seconds, annealing at 60°C for 30 seconds, and a total of 40 cycles. Each group consisted of three biological replicates. The relative expression was calculated by $2^{-\Delta\Delta C_t}$.

The primers for real-time fluorescence quantitative PCR were designed using Primer Premier 5.0 software based on the sequences of sheep genes available in the GenBank database. The primers were synthesized by Beijing HuadaGene Information Company (Table 1).

West-blot assay

Sheep GCs in different treatment groups were washed three times with PBS, and then RIPA cell lysis buffer was mixed with PMSF (100 : 1). Each well was added with 200 μ L, lysed on ice for 30 min, centrifuged at 15,000 r/min for 15 min, and the supernatant was collected. After the protein concentration was determined by BCA method, it was placed at -80°C for later use. The protein was mixed with 4 \times sodium dodecyl sulfate (SDS) loading buffer (3 : 1) and incubated in a boiling water bath at 100°C

Table 1. Real-time PCR primer sequences.

Gene	Primer sequence (5'-3')	Product size/bp	Accession number
<i>PCNA</i>	F-TCTTGAAGAAAGTGCTGGAGGC R-TCCGCATTATCTTCAGCCCTTA	259	XM_004014340.5
<i>Bcl-2</i>	F-ATGCCCTTTGTGGAGCTGTATGG R-ACTGAGCAGTGCCTTCAGAGACA	180	XM_027960877.2
<i>Bax</i>	F-GACAGGGGCCCTTTTGCTT R-TCAGACACTCGCTCAGCTTC	128	XM_027978592.2
<i>CAT</i>	F-TTACCAGATACTCCAAGGCGAAG R-AAAGGACGGAAACAGTAGAGCAT	221	XM_004016396.5
<i>SOD1</i>	F-CAATCACAGCATCTTCTGGACAAAT R-CCTGGTTAGAACAAGCAGCAATCT	215	NM_001280703.1
<i>β-HSD</i>	F-GGAGACATTCTGGATGAGCAG R-TCTATGGTGTGGTGTTGGA	209	XM_027961610.2
<i>CYP19A1</i>	F-ATGCTGGTGCTGAGTATGTGGT R-GCTGACAATCTTGAGGGTGTTG	192	NM_001123000.1
<i>NRF2</i>	F-CACTTCATCTGGCAGCAGATAT R-ACCACCTCTTGATGATTGTGTTCC	238	XM_042252469.1
<i>HO-1</i>	F-CAGGCCACCAAGTGCTATGT R-CAGGGCCTCTGAGCAATCT	141	XM_027967703.2
<i>Keap1</i>	F-TGCCCTGTGGTCAAAGTG R-GGTTCCGGTACCGTCCTGC	104	XM_015274015.1
<i>ACTIN</i>	F-ATATTGCTGCGCTCGTGGTT R-GTTGGTGACAATGCCGTGCT	224	NM_001009784.3

for 10 min to prepare protein separation gel (15%) and concentrated gel (5%), respectively. The sample was added to 10 µL protein/lane. After SDS-PAGE electrophoresis, the membrane was electrotransferred to polyvinylidene fluoride (PVDF) membrane, washed once with PBS, blocked with 5% skimmed milk powder solution at room temperature for 3 h, incubated with primary antibody overnight at 4°C, washed three times with PBST, 5 min each time, and added horseradish peroxidase-labeled secondary antibody (1 : 3000). After incubation at 37°C for 1 h, the PVDF membrane was washed three times with PBST for 5 min each time. The electrochemiluminescence solution was added to the PVDF membrane and incubated in the dark for 2 min. The chemiluminescence instrument was used for detection. Finally, the software ImageJ was used to detect the target band.

Statistical analysis

GraphPad Prism 8 software was used to analysis the data using one-way ANOVA, and the pairwise comparison was performed using the LSD and Tukey's test. The results were expressed as mean ± standard deviation.

Results

Isolation of GCs

The primary passage GCs that were cultured for 72 h had fully adherence (Figure 1a–c).

H₂O₂ reduces the viability of GCs cells

To find the optimal concentration of H₂O₂ for cell damage, this experiment treated GCs with different concentrations of H₂O₂ for varying durations (Figure 2a,b). Then apoptosis and apoptosis index Caspase-3 were verified by flow cytometry and Western blot (Figure 2c,d). The results showed that a treatment with 200 µM H₂O₂ for 12 hours reduced the cell proliferation rate to 50%. Therefore, subsequent experiments all used a treatment of 200 µM H₂O₂ for 12 hours on GCs.

NAC enhance the antioxidant capacity of H₂O₂ on GCs

The impact of NAC on ROS levels in GCs was evaluated. Compared with the H₂O₂ treatment group, the NAC and H₂O₂ co-treatment group significantly decreased the levels of ROS (Figure 3a,b). The antioxidant-related gene catalase (CAT) and superoxide dismutase 1 (SOD1) were assessed by RT-PCR. Compared with the H₂O₂ treatment group, the NAC and H₂O₂ co-treatment group significantly up-regulated the expression of CAT and SOD1 (Figure 3c,d).

NAC attenuate the oxidative stress damage of H₂O₂ on GCs

The effect of NAC on oxidative stress indicators of sheep GCs induced by H₂O₂ was explored. Compared with the H₂O₂ treatment group, the NAC and H₂O₂ co-treatment group significantly increased the content of

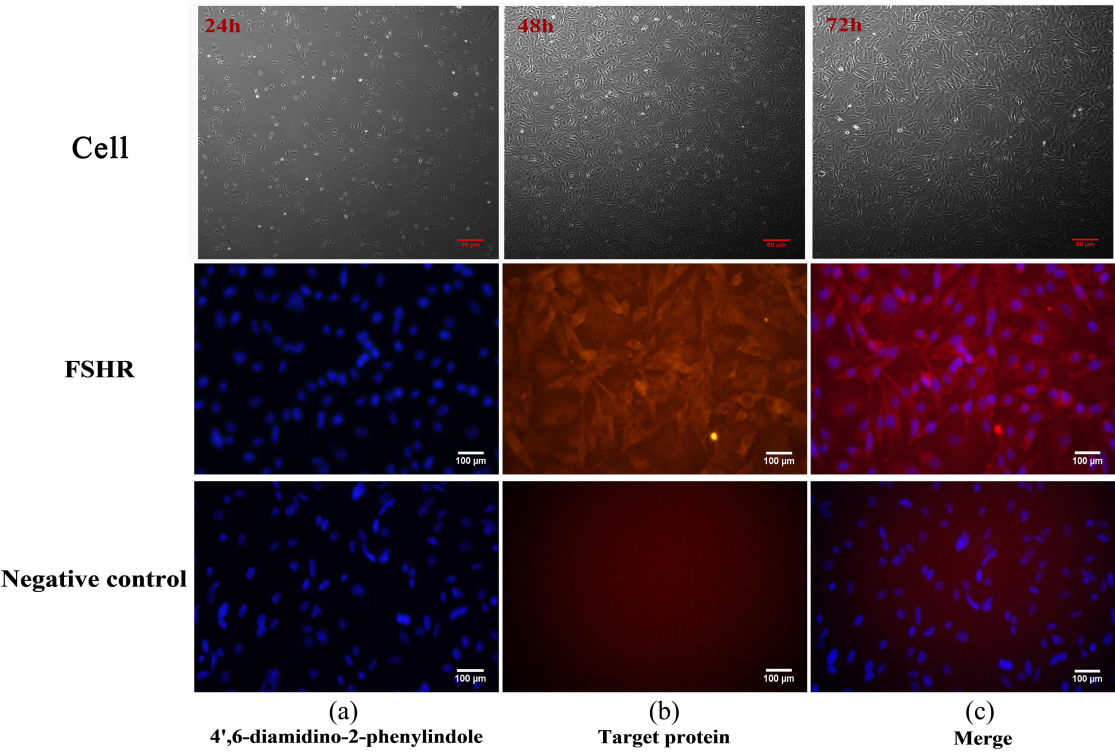


Figure 1. Immunofluorescence images : the growth status of cells at 12 hours, 48 hours, and 72 hours and the immunofluorescence staining images of FSHR.

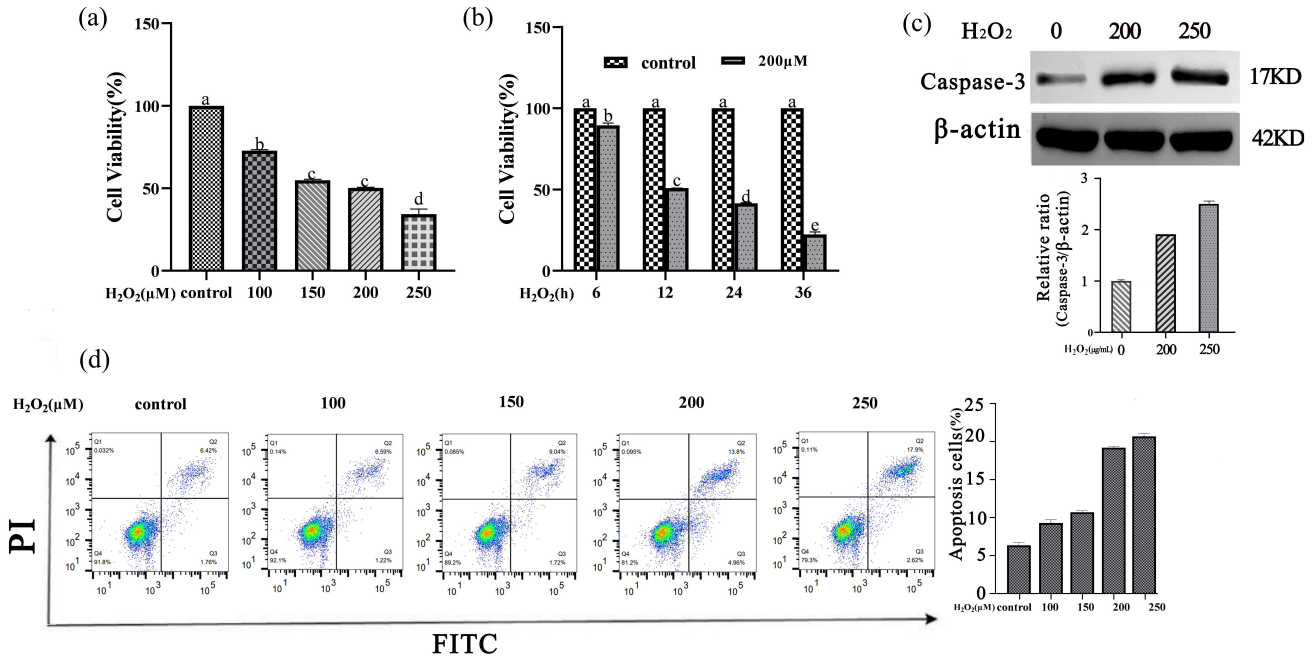


Figure 2. CCK-8, WB and flow cytometry : validation of H2O2-induced GCs apoptosis.

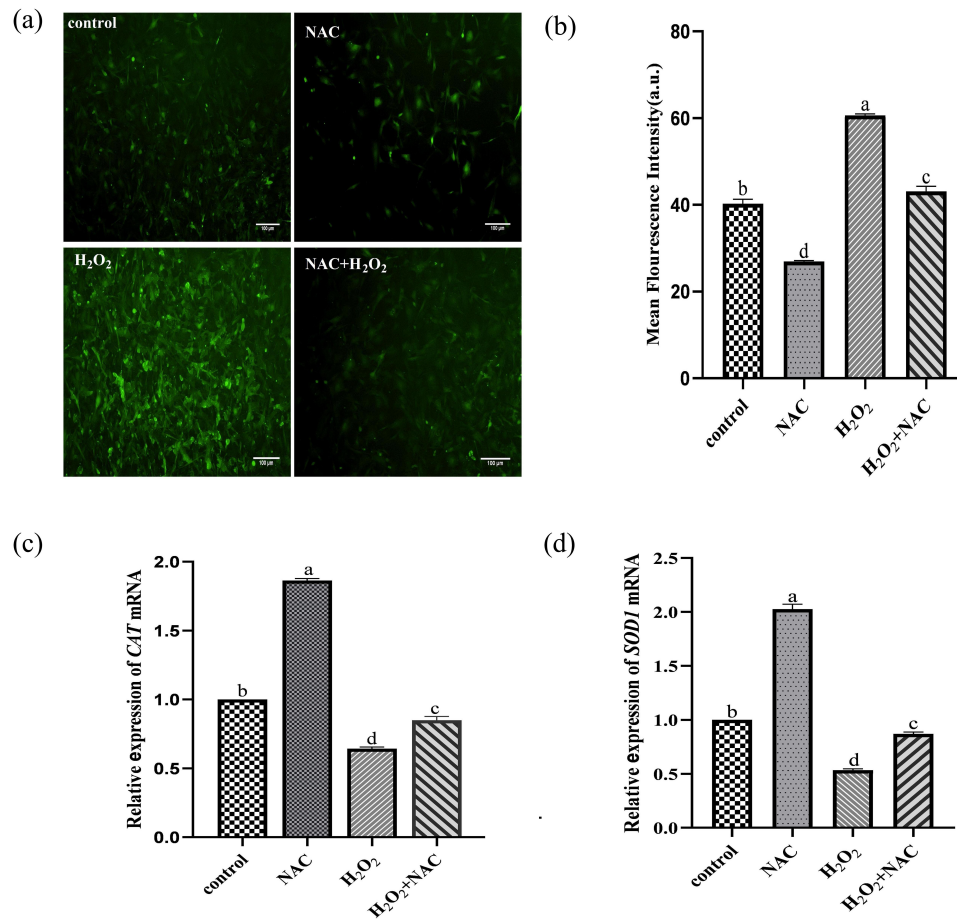


Figure 3. Reactive oxygen species staining and RT-PCR results : the effect of NAC on ROS levels in GCs was evaluated.

GSH and the activity of SOD ($p < .01$), and decreased the content of MDA (Figure 4).

NAC inhibit the apoptosis of H₂O₂ on GCs

The molecular mechanism of NAC on apoptosis was investigated by measuring the expression levels of apoptosis-related genes (*Bcl-2* and *Bax*) by qRT-PCR. The results showed that the expression levels of *Bcl-2* were significantly upregulated, *Bax* was significantly down-regulated in the NAC combined with H₂O₂ group than in the H₂O₂ group (Figure 5a–b). The expression levels of *Bcl-2* and *Bax* proteins were detected by Western blot and immunofluorescence staining (Figure 5c–g). The results showed that *Bcl-2* and *Bax* were consistent with the changes in its genes expression.

NAC can promote the proliferation of sheep GCs under oxidative stress

NAC significantly increased the proliferation activity of GCs (Figure 6a) in the NAC combined with H₂O₂

group than in the H₂O₂ group. The proliferation related genes (*PCNA*) was investigated by qRT-PCR. *PCNA* genes expression levels were significantly up-regulated (Figure 6b) in the NAC combined with H₂O₂ group than in the H₂O₂ group.

NAC promote steroid hormone secretion of H₂O₂ on GCs

The level of steroid hormone secretion was assessed by ELISA for progesterone and androgen content in the culture medium supernatant. The secretion of E₂ and P₄ were increased significantly (Figure 7a–b) in the NAC combined with H₂O₂ group than in the H₂O₂ group. The molecular mechanism was investigated by measuring the expression levels of steroidogenesis-related genes (*CYP19A1* and *3β-HSD*) by qRT-PCR. The results showed that the *CYP19A1* and *3β-HSD* were significantly upregulated (Figure 7c–d) in the NAC combined with H₂O₂ group than in the H₂O₂ group.

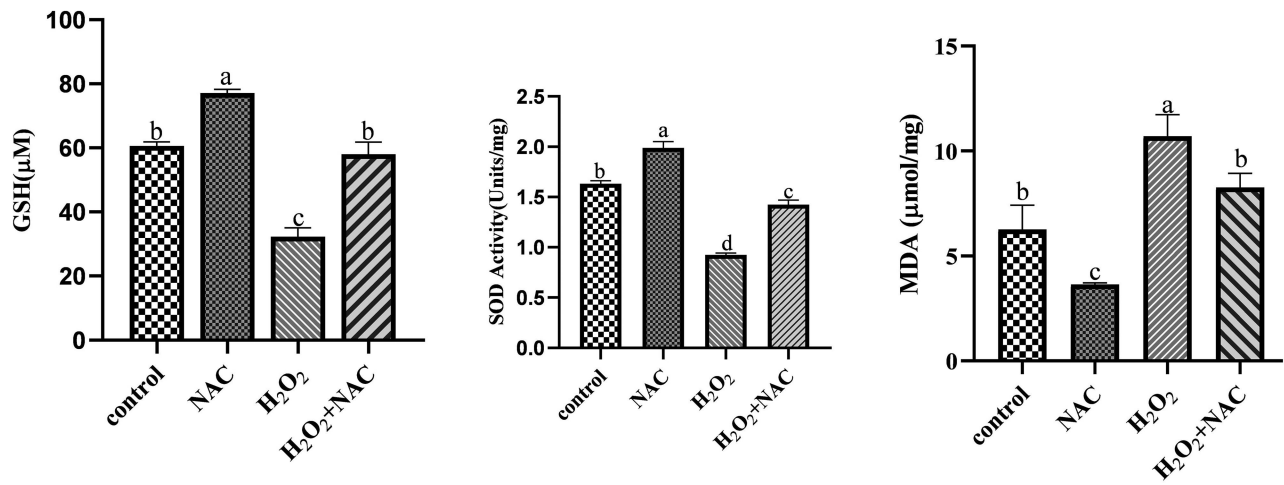


Figure 4. ELISA assay picture: the effect of NAC on oxidative stress indicators of sheep GCs induced by H₂O₂ was explored.

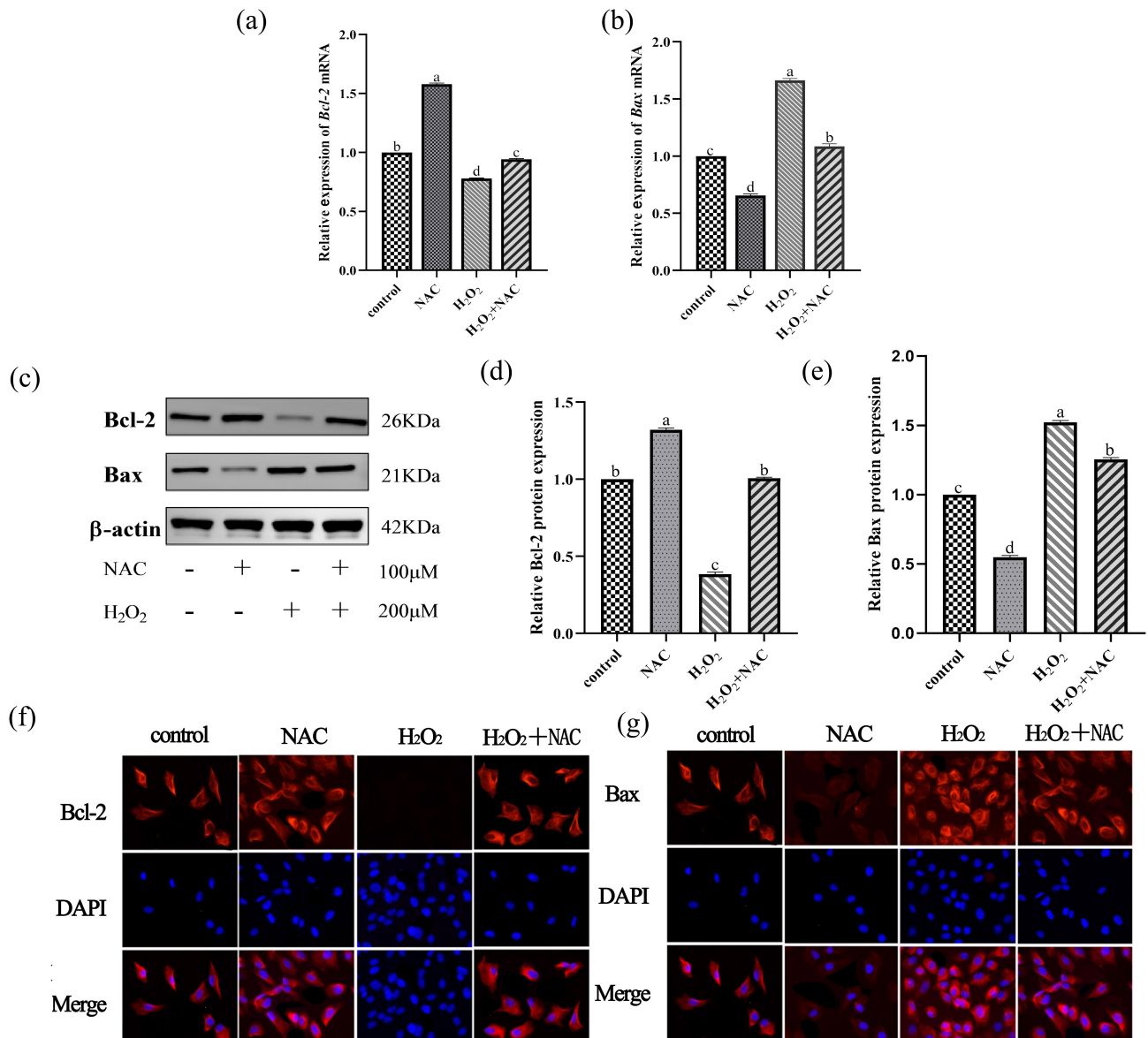


Figure 5. RT-PCR, WB and immunofluorescence images: to verify the effect of NAC on H₂O₂-induced GCs apoptosis in sheep.

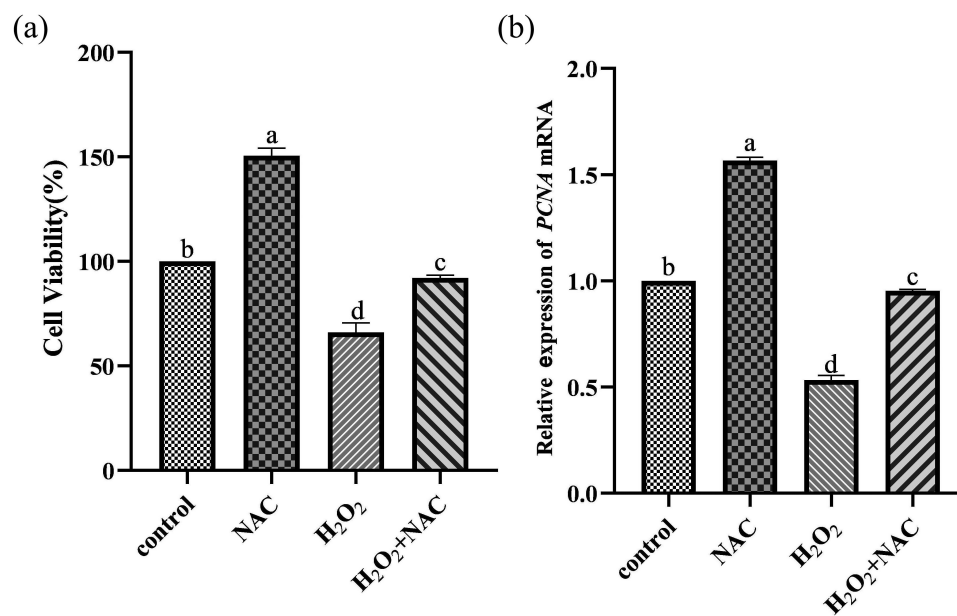


Figure 6. RT-PCR and CCK-8 images: NAC can promote the proliferation of sheep GCs under oxidative stress.

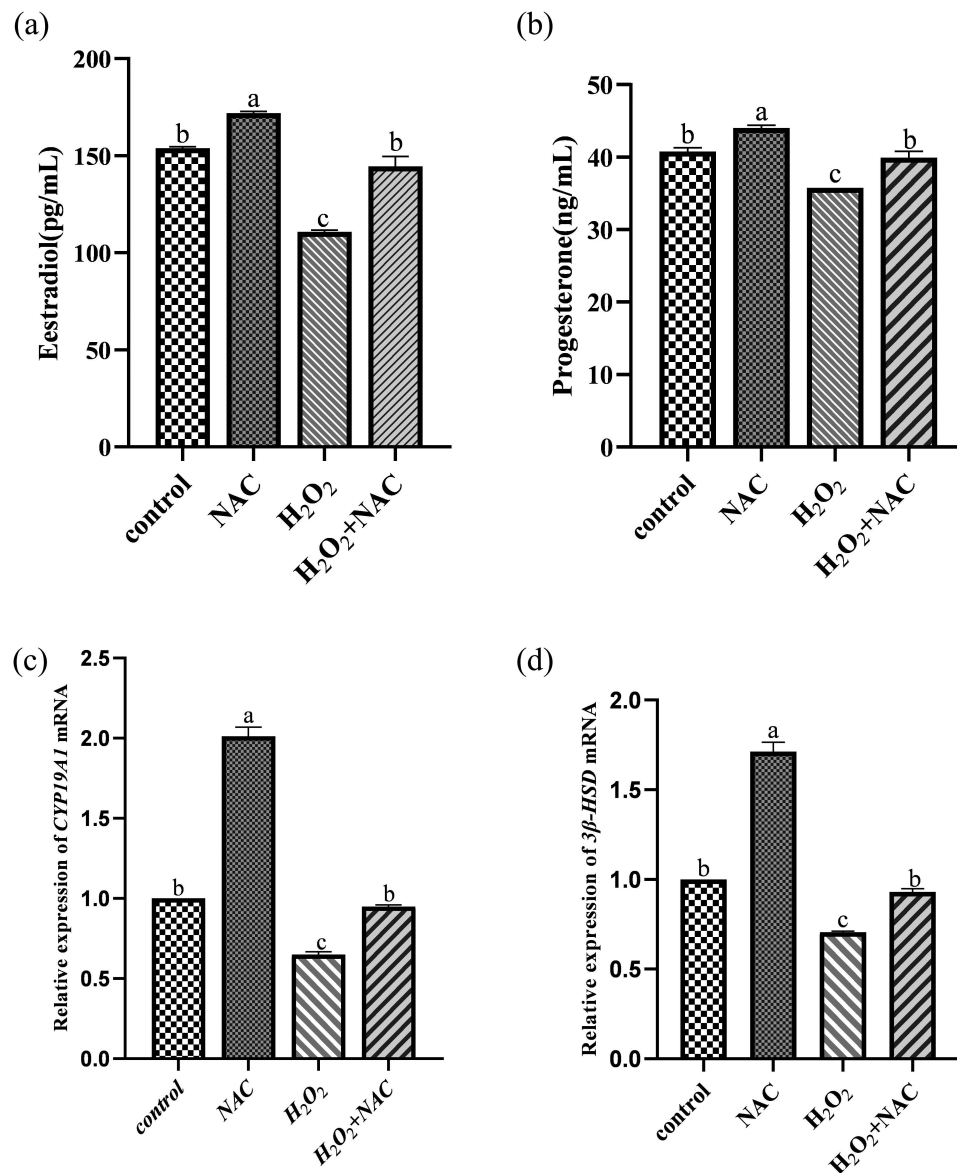


Figure 7. ELISA and qRT-pcr results: NAC promoted steroid hormone secretion of H₂O₂ on GCs.

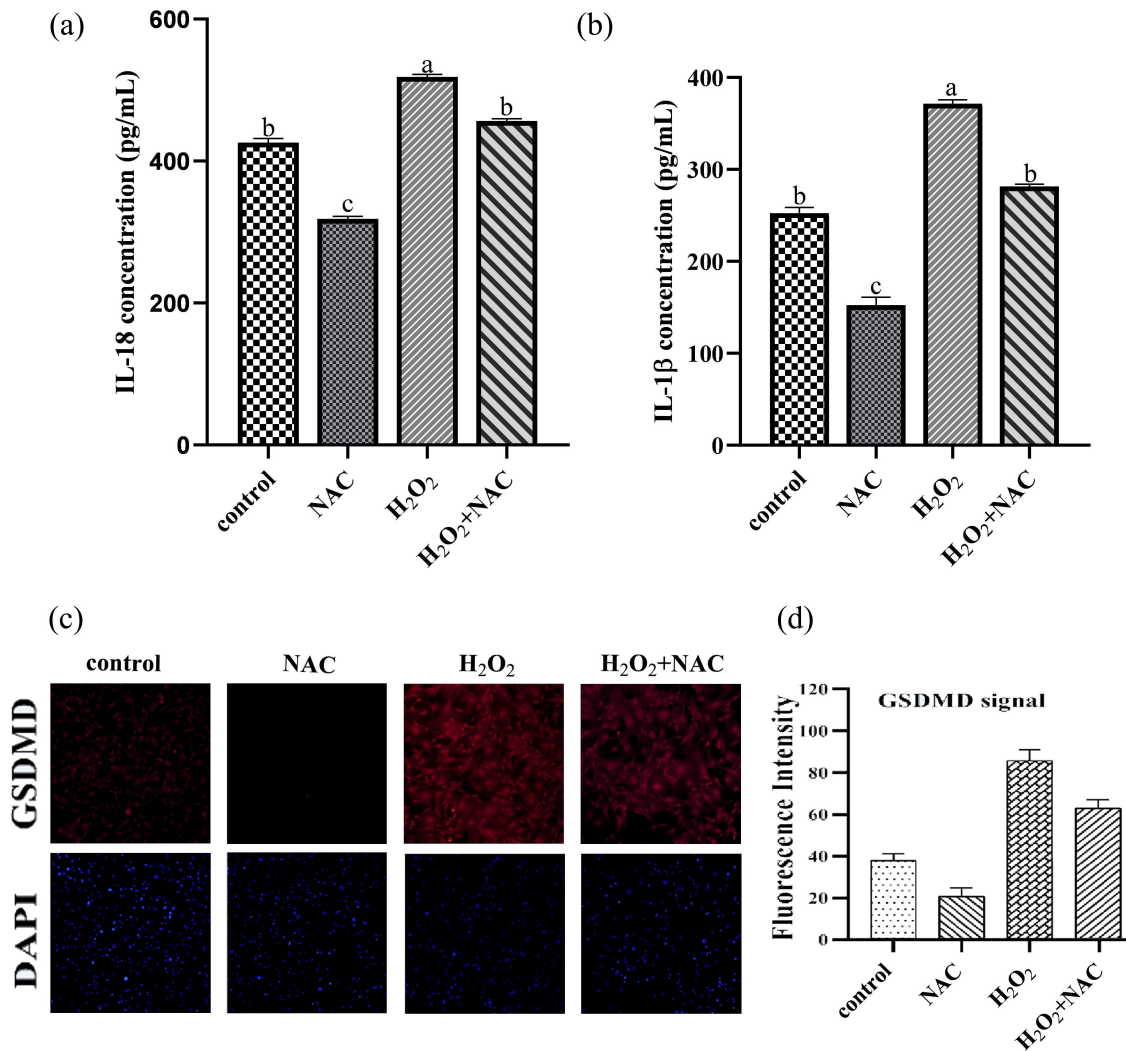


Figure 8. Results of ELISA and immunofluorescence: NAC inhibited the inflammation of H₂O₂ on GCs.

NAC inhibit inflammation of H₂O₂ on GCs

ELISA and immunofluorescence staining showed that NAC combined with H₂O₂ significantly reduced IL-18, IL-1 and GSDMD in the supernatant ($p < .05$) (Figure 8a–d).

NAC alleviates of H₂O₂ on GCs through NRF2/HO-1 and PI3K/AKT signal pathways

Compared with NAC and H₂O₂ treatment groups, NAC and H₂O₂ co-treatment groups significantly up-regulated the mRNA levels of *NRF2* and *HO-1* genes and down-regulated the mRNA level of *Keap-1* gene (Figure 9a–c). Compared with NAC and H₂O₂ groups, the expression levels of *NRF2* and *HO-1* protein in NAC and H₂O₂ co-treatment groups were significantly increased ($p < .05$) (Figure 9d–f). Compared with NAC and H₂O₂ groups, the expression levels of p-PI3K/PI3K

and p-Akt/Akt in NAC and H₂O₂ co-treatment groups were significantly increased ($p < .05$) (Figure 9g–i).

Discussion

Female mammals experience stress from lactation and pregnancy, which can lead to excessive production of ROS [18], primarily including superoxide anion radical ($O_2^{\cdot-}$), hydroxyl radical (OH^{\cdot}), and H₂O₂. Oxidative stress adversely affects the health and reproductive performance of female animals [19]. Among various causes of reproductive disorders in sheep, H₂O₂ is a key factor in inducing oxidative stress [20]. It is crucial to explore oxidative stress and the mechanisms related to H₂O₂, a reactive oxygen species molecule that can increase intracellular ROS and cause cellular damage [21]. H₂O₂ is commonly used to quickly establish cell oxidative stress injury models.

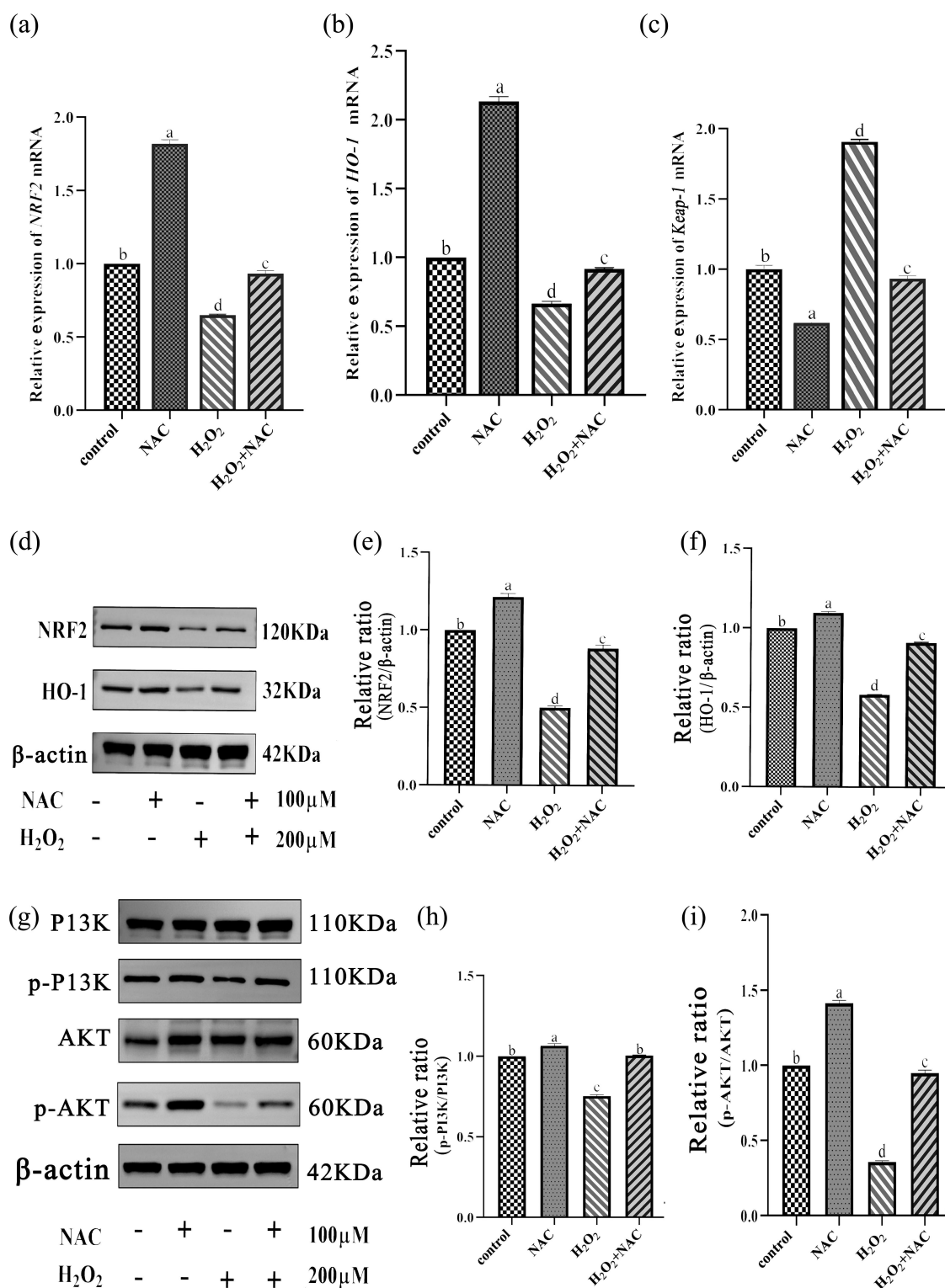


Figure 9. Results of qRT-PCR and WB: to verify the effect of NAC on H₂O₂-induced GCs antioxidant signaling pathway.

Cell proliferative activity is an essential indicator for assessing the in vitro proliferation capacity of cells under different treatment conditions [22]. In this study, 200 μ mol/L H₂O₂ treatment for 12 hours resulted in a cell survival rate of 50.29%, indicating

that GCs were somewhat damaged but retained some proliferative and differentiative abilities. Therefore, this concentration and duration of H₂O₂ exposure were chosen to construct the GCs oxidative damage model.

Oxidative stress can impair follicular GC function, leading to poor oocyte quality and reduced reproductive performance in mammals [23]. H_2O_2 treatment increased ROS levels in GCs [24], elevated malondialdehyde (MDA) content, and decreased glutathione (GSH) content and SOD activity. N-acetylcysteine (NAC), an antioxidant, can mitigate H_2O_2 effects on GCs by scavenging ROS, reducing MDA content, and increasing SOD activity [25]. Studies have demonstrated that NAC can inhibit oxidative stress-induced apoptosis in various cell types, promote oocyte maturation, and improve early embryonic development by modulating ROS and GSH levels [26].

During follicular development, the proliferation of GCs is crucial for oocyte growth and ovarian function [27]. H_2O_2 treatment significantly inhibited GC proliferation and induced apoptosis, while NAC pretreatment significantly mitigated these adverse effects. NAC may promote GC proliferation by increasing the level of the *PCNA* gene, a marker of cell proliferation and important for cell cycle regulation [28].

Furthermore, quantitative RT-PCR showed that NAC treatment significantly upregulated the anti-apoptotic gene *Bcl-2* and downregulated the pro-apoptotic gene *Bax*. GC apoptosis is a key factor in follicular atresia, a selective process in mammalian folliculogenesis. NAC has been shown to attenuate oxidative stress-induced apoptosis by modulating pathways such as *Bax*/Caspase-3 [29].

In mammalian follicular development, GCs surround oocytes, providing nutrition and secreting hormones. H_2O_2 treatment significantly reduced the secretion of P_4 and E_2 by GCs, but NAC pretreatment followed by H_2O_2 exposure significantly increased P_4 and E_2 secretion. The expression of steroidogenesis-related genes *CYP19A1* and *3 β -HSD* was also upregulated by NAC pretreatment, indicating a positive effect of NAC on steroid hormone secretion by sheep GCs under oxidative stress [30].

Oxidative stress can promote inflammation. NAC has been shown to inhibit apoptosis and inflammatory responses induced by various stressors in different cell types and to improve inflammatory conditions. In this experiment, the levels of inflammatory cytokines IL-18 and IL-1 β increased with H_2O_2 treatment but significantly decreased after NAC pretreatment and H_2O_2 exposure, suggesting that NAC can effectively reduce the levels of these inflammatory factors in an oxidative stress model [31].

NRF2 is involved in the cellular response to oxidative stress, and its signaling pathway regulates metabolic and antioxidant enzymes. Under oxidative stress, NRF2 dissociates from its inhibitor Keap1 and translocates to

the nucleus to regulate the transcription of antioxidant genes such as *HO-1*. The phosphatidylinositol 3-kinase (PI3K)/Akt pathway is an upstream signal of NRF2 and plays a protective role against oxidative stress. NAC has been shown to activate the PI3K/Akt signaling pathway, which in turn activates NRF2/HO-1 signaling, protecting cells from apoptosis and improving oocyte quality.

In conclusion

The oxidative damage model was successfully constructed by 200 μ mol/L H_2O_2 for 12 h. It was found that NAC could protect the proliferation of GCs and reduce the content of ROS and MDA under H_2O_2 -induced oxidative stress. Increase GSH content and SOD activity. Reduce cell apoptosis and inflammatory factors IL-18, IL-1 content; up-regulate the protein of *Bcl-2*, down-regulate the expression level of *Bax* gene and protein; inhibition of NRF2 and HO-1 gene and protein expression; promote the secretion of E_2 and P_4 by granulosa cells. The molecular mechanism may be that NAC alleviates H_2O_2 -induced oxidative stress injury through NRF2 and PI3K/AKT signaling pathways.

Disclosure statement

No potential conflict of interest was reported by the author(s).

Funding

This research was supported by the National Natural Science Foundation of China [32460907], Lanzhou Science and Technology Plan Project [No. 20222-44], and Innovative Team for Animal Diseases in Plateau [20240036].

Authors' contributions

Hao Chen: designed the study, performed the experiments, wrote the original draft, curated the manuscript. **Jine Wang:** designed the study, performed the experiments, wrote the original draft, curated the manuscript. **Bingzhu Zhao:** performed the experiments, wrote the original draft, and curated the manuscript. **Yahua Yang:** helped in performing the experiments, formal analysis, and data curation. **Chongfa Yang:** helped in writing – review & editing, the manuscript, formal analysis, and data curation. **Zhijie Zhao:** performed the experiments, writing-original draft, and curated the manuscript. **Xiaona Ding:** performed the experiments, writing-original draft, and curated the manuscript. **Taojie Zhang:** helped in performing the experiments, formal analysis, and data curation. **Yang Li:** designed the study and helped in writing-original draft, and curated the manuscript. **Zhaxi Yingpai:** helped in performing the experiments, formal analysis, and data curation. **Shengdong Huo:** designed the study and helped in writing-original draft, and manuscript curation. All authors have read and approved the manuscript.

Author statement

All authors have read and approved the final version of the manuscript.

Data availability statement

The datasets used and/or analyzed during the current study are available from the corresponding author on reasonable request.

ORCID

Hao Chen  <http://orcid.org/0009-0007-2630-7587>

References

- [1] Siddiqui S, Mateen S, Ahmad R, et al. A brief insight into the etiology, genetics, and immunology of polycystic ovarian syndrome (PCOS). *J Assist Reprod Genet.* 2022;39(11):2439–2473. doi: 10.1007/s10815-022-02625-7
- [2] Cheung EC, Vousden KH. The role of ROS in tumour development and progression. *Nat Rev Cancer.* 2022;22(5):280–297. doi: 10.1038/s41568-021-00435-0
- [3] Chen E, Wang T, Tu Y, et al. Ros-scavenging biomaterials for periodontitis. *J Mater Chem B.* 2023;11(3):482–499. doi: 10.1039/D2TB02319A
- [4] Kim EJ, Yang C, Lee J, et al. The new biocompatible material for mouse ovarian follicle development in three-dimensional in vitro culture systems. *Theriogenology.* 2020;144:33–40. doi: 10.1016/j.therio.2019.12.009
- [5] Canat A, Atilla D, Torres-Padilla ME. Hyperosmotic stress induces 2-cell-like cells through ROS and ATR signaling. *EMBO Rep.* 2023;24(9):e56194. doi: 10.15252/embr.202256194
- [6] Zhang S, Liu Q, Chang M, et al. Chemotherapy impairs ovarian function through excessive ros-induced ferroptosis. *Cell Death Dis.* 2023;14(5):340. doi: 10.1038/s41419-023-05859-0
- [7] Stosik MP, Tokarz-Deptuła B, Deptuła W. Melanomacrophages and melanomacrophage centres in Osteichthyes. *Cent Eur J Immunol.* 2019;44(2):201–205. doi: 10.5114/ceji.2019.87072
- [8] Huo S, Chen Z, Li S, et al. A comparative transcriptome and proteomics study of post-partum ovarian cycle arrest in yaks (*Bos grunniens*). *Reprod Domest Anim.* 2022;57(3):292–303. doi: 10.1111/rda.14059
- [9] Chen Z, Wang J, Ma J, et al. Transcriptome and proteome analysis of pregnancy and postpartum anoestrus ovaries in yak. *J Vet Sci.* 2022;23(1):e3. doi: 10.4142/jvs.21195
- [10] Wang Y, Yang C, Elsheikh NAH, et al. HO-1 reduces heat stress-induced apoptosis in bovine granulosa cells by suppressing oxidative stress. *Aging (Albany NY).* 2019;11(15):5535–5547. doi: 10.18632/aging.102136
- [11] An R, Wang X, Yang L, et al. Polystyrene microplastics cause granulosa cells apoptosis and fibrosis in ovary through oxidative stress in rats. *Toxicology.* 2021;449:152665. doi: 10.1016/j.tox.2020.152665
- [12] Kumar P, Osahon OW, Sekhar RV. GlyNAC (glycine and N-acetylcysteine) supplementation in mice increases length of life by correcting glutathione deficiency, oxidative stress, mitochondrial dysfunction, abnormalities in mitophagy and nutrient sensing, and genomic damage. *Nutrients.* 2022;14(5):14. doi: 10.3390/nu14051114
- [13] Zhao H, Huang J, Li Y, et al. Ros-scavenging hydrogel to promote healing of bacteria infected diabetic wounds. *Biomaterials.* 2020;258:120286. doi: 10.1016/j.biomaterials.2020.120286
- [14] Ji T, Chen X, Zhang Y, et al. Effects of N-Acetylcysteine on the proliferation, hormone secretion level, and gene expression profiles of goat ovarian granulosa cells. *Genes (Basel).* 2022;13(12):2306. doi: 10.3390/genes13122306
- [15] Pedre B, Barayeu U, Ezeriņa D, et al. The mechanism of action of N-acetylcysteine (NAC): the emerging role of H (2)S and sulfane sulfur species. *Pharmacol & Ther.* 2021;228:107916. doi: 10.1016/j.pharmthera.2021.107916
- [16] Tang ZL, Zhang K, Lv SC, et al. LncRNA MEG3 suppresses PI3K/AKT/mTOR signalling pathway to enhance autophagy and inhibit inflammation in tnfr-α-treated keratinocytes and psoriatic mice. *Cytokine.* 2021;148:155657. doi: 10.1016/j.cyto.2021.155657
- [17] Hu X, Xu Q, Wan H, et al. PI3K-Akt-mTOR/PFKFB3 pathway mediated lung fibroblast aerobic glycolysis and collagen synthesis in lipopolysaccharide-induced pulmonary fibrosis. *Lab Invest.* 2020;100(6):801–811. doi: 10.1038/s41374-020-0404-9
- [18] Yang Y, Chen Z, Yang C, et al. Calcium promoting maturity of oocytes through calcium/calmodulin-dependent protein kinase II of yak (*Bos grunniens*). *Ital J Anim Sci.* 2024;23(1):895–906. doi: 10.1080/1828051X.2024.2358869
- [19] Razavi SM, Soltan MS, Abbasian K, et al. Host oxidative stress in piroplasmosis: a review in domestic animals. *Vet Parasitol.* 2023;322:110011. doi: 10.1016/j.vetpar.2023.110011
- [20] Flahaut S, Laplace JM, Frère J, et al. The oxidative stress response in *Enterococcus faecalis*: relationship between H₂O₂ tolerance and H₂O₂ stress proteins. *Lett Appl Microbiol.* 1998;26(4):259–264. doi: 10.1046/j.1472-765X.1998.00325.x
- [21] Varisli L, Tolan V. Increased ROS alters E-/n-cadherin levels and promotes migration in prostate cancer cells. *Bratisl Lek Listy.* 2022;123:752–757. doi: 10.4149/BLL_2022_121
- [22] Kato TA, Haskins JS. Mitotic index analysis. In: *Methods in molecular biology.* Vol. 2519. Clifton, NJ; 2023. p. 17–26.
- [23] Shen M, Jiang Y, Guan Z, et al. FSH protects mouse granulosa cells from oxidative damage by repressing mitophagy. *Sci Rep.* 2016;6(1):38090. doi: 10.1038/srep38090
- [24] Yang Z, Hong W, Zheng K, et al. Chitosan oligosaccharides alleviate H₂O₂-stimulated granulosa cell damage via HIF-1α signaling pathway. *Oxid Med Cell Longev.* 2022;2022:1–15. doi: 10.1155/2022/4247042
- [25] Ma J, Wang J, Hu S, et al. Effects of melatonin on development and hormone secretion of sheep theca

- cells in vitro. *Theriogenology*. 2023;198:172–182. doi: [10.1016/j.theriogenology.2022.12.036](https://doi.org/10.1016/j.theriogenology.2022.12.036)
- [26] Luo Z, Xu X, Sho T, et al. Ros-induced autophagy regulates porcine trophectoderm cell apoptosis, proliferation, and differentiation. *Am J Physiol Cell Physiol*. 2019;316(2):C198–c209. doi: [10.1152/ajpcell.00256.2018](https://doi.org/10.1152/ajpcell.00256.2018)
- [27] Baumgarten SC, Armouti M, Ko C, et al. IGF1R expression in ovarian granulosa cells is essential for steroidogenesis, follicle survival, and fertility in female mice. *Endocrinology*. 2017;158(7):2309–2318. doi: [10.1210/en.2017-00146](https://doi.org/10.1210/en.2017-00146)
- [28] Mansour FR, Nabiuni M, Amini E. Ovarian toxicity induced by aluminum chloride: alteration of Cyp19a1, PCNA, Puma, and Map1lc3b genes expression. *Toxicology*. 2022;466:153084. doi: [10.1016/j.tox.2021.153084](https://doi.org/10.1016/j.tox.2021.153084)
- [29] Zhao K, Han D, He SR, et al. N-acetyl-L-cysteine attenuates oxidative stress-induced bone marrow endothelial cells apoptosis by inhibiting BAX/caspase 3 pathway. *Biochem Biophys Res Commun*. 2023;656:115–121. doi: [10.1016/j.bbrc.2023.03.045](https://doi.org/10.1016/j.bbrc.2023.03.045)
- [30] Mohammadi-Bardbori A, Omidi M, Arabnezhad MR. Impact of CH223191-induced mitochondrial dysfunction on its aryl hydrocarbon receptor agonistic and antagonistic activities. *Chem Res Toxicol*. 2019;32(4):691–697. doi: [10.1021/acs.chemrestox.8b00371](https://doi.org/10.1021/acs.chemrestox.8b00371)
- [31] Zhou LH, Zou H, Hao JY, et al. Metformin inhibits ovarian granular cell pyroptosis through the miR-670-3p/NOX2/ROS pathway. *Aging (Albany NY)*. 2023;15(10):4429–4443. doi: [10.18632/aging.204745](https://doi.org/10.18632/aging.204745)